Proceedings of Science and Mathematics
Faculty of Science, Universiti Teknologi Malaysia

Vol. 16, 2023, page 117 – 127

Two-Dimensional Model for Solute Transport Induced by Groundwater Abstraction

Farah Nur Atikah Mior Othman, Shaymaa Mustafa*
Department of Mathematical Sciences, Faculty of Science, Universiti Teknologi Malaysia
*Corresponding author: mdshaymaa@utm.my

Abstract
Groundwater extraction is frequently used in a water resource management. This paper offers an analytical model of solute transport to examine the possibility of groundwater contamination by pollution sources close to the pumping well. Advection Dispersion Equation was used to generate the analytical solution, which was then solved using Green's Function. These methods were used in an aquifer that the river partially drained, and they were sufficiently universal to be used in both confined and unconfined aquifers. At first, it is believed that the aquifer is uncontaminated. MATLAB software was used to plot the analytical solution that was obtained using Green's Function. The model quantifies the transport of solutes in the aquifer and predicts their fate and concentration distribution under varying abstraction scenarios. It considers different parameters such as pumping rates, abstraction well locations, pumping time, and aquifer thickness to explore their effects on pollutant concentration. The results from MATLAB are presented graphically and thoroughly examined. According to the findings, the contamination around the well increased with increasing values for these parameters. If the maximum allowable concentration of a particular pollutant in raw water is known, the model can be used to determine the best pumping rate and well site for that contaminant.

Keywords: Analytical solutions; Solute transport; Groundwater; Pumping well; Green's function; Contamination

1. Introduction

According to a website from National Geographic, we use a significant amount of groundwater for domestic, industrial, and agricultural purposes. Aquifers are where the majority of groundwater is found, including a sizable percentage of our drinking water. Springs, lakes, rivers, streams, and artificial wells are all ways to release existing groundwater. It is replenished by rainfall, snowfall, or seepage of water from other sources, such as irrigation and water supply system leaks.

By extracting groundwater, the number of contaminants that migrate away from the well and the size of the contaminated area is both limited. This becomes crucial when contaminants cross boundaries or enter drinking water aquifers, rivers, lakes, streams, or seas. According to an online website from QED Environmental Systems, groundwater extraction is carried out by pumping water from the well to remove water and any dissolved or floating impurities from inside the well. Because the rate of river water seepage is relatively slow and the aquifer contains biological processes, the water extracted from the well exhibits superior quality compared to the river water (Mustafa et al., 2021).

Numerous researchers prefer the use of analytical solute transport models because they can offer a deeper understanding of contaminant transport mechanisms and better forecasts of solute plume migration (Mustafa et al., 2021). The Green's Function, an analytical method widely utilized by numerous researchers, is commonly employed to address solute transport models. Secomb (2015) employed the Green's Function methodology to model the movement of reactive solutes within microvascular networks and the adjacent tissues, taking into account both convective and diffusive mechanisms. In this methodology, the solute concentration distribution within the tissue is expressed as a composite of spatial fields created by varying distributions of distinct sources and sinks over time. Furthermore, in a parallel fracture-matrix system, Chen and Zhan (2018) employed a novel approach based on Green's function to address the problem of two-dimensional solute transport.

2. Mathematical Formulation

The developed model simulates the movement of pollutants in the direction of a pumping well from a river (Fig. 4.1). Two main assumptions were made in the model: (1) The flow is assumed to be uniform in the x-direction, with specified hydraulic head values at the left and right domain boundaries, and (2) no specific flow boundary circumstances are assigned to the boundaries in the northern and southern domains. In a previous study conducted by Libera et al. in 2017, it was assumed that the pumping rate of the well, Q$\left(\frac{L^3}{T}\right)$ remains unchanged, and the aquifer exhibits homogeneity, isotropy, and has a finite depth of d.

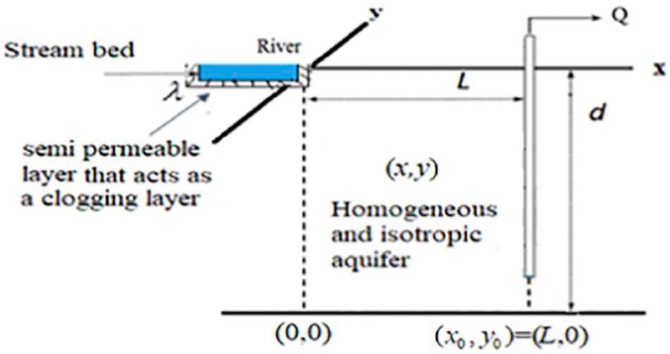

Figure 1 Schematic depiction of the pumping well from the river

To develop a two-dimensional analytical solution for contaminant transport in groundwater system, the two-dimensional ADE for contaminant transport in uniform flow is formulated as below:

$$R\frac{\partial C}{\partial t} = D_x\frac{\partial^2 C}{\partial x^2} + D_y\frac{\partial^2 C}{\partial y^2} - U_x\frac{\partial C}{\partial x} - vRC \tag{1}$$

By moving the right-hand side (RHS) of the Equation 4.1 to the left-hand side (LHS) will provide the following equation:

$$R\frac{\partial C}{\partial t} - D_x\frac{\partial^2 C}{\partial x^2} - D_y\frac{\partial^2 C}{\partial y^2} + U_x\frac{\partial C}{\partial x} + vRC = 0 \tag{2}$$

where

$C(x, y, t)$: concentrations of contaminant, (M/L^3)
D_x : components of longitudinal and transverse dispersion coefficient along the x-axis, (L^2/T)
D_y : components of longitudinal and transverse dispersion coefficient along the y-axis, (L^2/T)
U_x : seepage velocity, (L/T)
v : decay constant, $(1/T)$
R : linear retardation factor
$D_x = a_l U_x$: dispersion coefficient along x-axis
$D_y = a_t U_x$: dispersion coefficient along y-axis
a_l : longitudinal and transverse dispersivity along the x-axis, (L)
a_t : longitudinal and transverse dispersivity along the y-axis, (L)

when $\beta = \upsilon R$ is substituted, then we will have:

$$R\frac{\partial C}{\partial t} - D_x\frac{\partial^2 C}{\partial x^2} - D_y\frac{\partial^2 C}{\partial y^2} + U_x\frac{\partial C}{\partial x} + \beta C = 0 \quad (3)$$

given that β is the degradation rate of the contaminants $(1/T)$.

To illustrate the extent of pollutant penetration within the aquifer and the reduction in concentration due to bacterial activity, the functions $C_{in}(x, y, t)$ and $C_{ads}(x, y, t)$ were utilized. Using a balanced equation, we get:

$$C_{in} - C_{ads} = C_w \quad (4)$$

If $C_w(t) = 0$ is equal to zero, the water extracted from the pumping well can be directly used as public drinking water without any additional treatment. Otherwise, if $C_w(t) = 0$ is not zero, which is usually the case, further treatment is required before the water can be distributed. The extent of filtration and the amount of pollutants in the pumped water determine the specific treatment processes needed at this stage. Hence equation 3 can be modified as shown below:

$$R\frac{\partial C}{\partial t} - D_x\frac{\partial^2 C}{\partial x^2} - D_y\frac{\partial^2 C}{\partial y^2} + U_x\frac{\partial C}{\partial x} + \beta C = -C_w(t)\delta(x - x_0)\delta(y - y_0) \quad (5)$$

Along with the initial and boundary conditions listed below:

$$C(x, y, t) = 0 \quad x \to \infty, -\infty \le y \le \infty \; and \; t \ge 0 \quad (6)$$

$$C(x, y, t) = 0 \quad y \to \pm\infty, -\infty \le x \le \infty \; and \; t \ge 0 \quad (7)$$

$$C(x, y, t) = S_0 f(t, y) \quad x = 0, -M \le y \le M \; and \; t \ge 0 \quad (8)$$

$$C(x, y, 0) = 0 \quad 0 < x < \infty, -\infty \le y \le \infty \; and \; t = 0 \quad (9)$$

where

δ : dimensionless Dirac delta function

M : length of the river that is under the effect of pumping well

$S_0(M/L^3.T))$: initial mass of contaminants dissolved in one unit volume of water within one unit of time

$f(t, y)$: a function of t and y which means that the river is not a uniform source of contaminant

An assumption is made that adsorption with a proportional isotherm will lower the amount of the pollutants transported from the river. As a result, $C_w(t)$ from Equation 4 is computed using the formula below:

$$C_w(t) = \frac{q}{Q\, S_0 \exp\left(-\beta t/R\right)} \quad (10)$$

given that

q: stream depletion flow rate $(L^3\, /T)$ that represented the overall flow out of the incompressible streambed

$\frac{q}{Q}$: proportion of infiltrated river water in the pumping well

By applying the modifications listed below:

$$\bar{x} = x - \frac{U_x t}{R};$$

$$\bar{C}(x,y,t) = c(x,y,t)\exp\left(\frac{\beta t}{R}\right);$$

$$C_0 = S_0 \frac{d}{U_x}$$

and $\bar{C}_w(t) = C_W(t)\exp\left(\frac{\beta t}{R}\right)\delta(x - x_0)\delta(y - y_0)$

And the following dimensionless:

$$t_D = \frac{U_x t}{d};$$

$$C_D(x,y,t) = \frac{\bar{C}(x,y,t)}{C_{0;}};$$

$$C_{wD}(t) = 1/(S_0 R)\bar{C}_w(t);$$

$$x_D = \bar{x}\sqrt{\frac{U_x R}{dD_x}} y_D = y\sqrt{\frac{U_x R}{dD_y}}$$

and $M_D = M\sqrt{\frac{U_x R}{dD_y}}$;.

Equations 4.5 - 4.9 then change into :

$$\frac{\partial c_D}{\partial t_D} - \frac{\partial^2 c_D}{\partial x^2{}_D} - \frac{\partial^2 c_D}{\partial y^2{}_D} = -C_{wD}(t_D) \tag{11}$$

$$C_D(x_D, y_D, t_D) \to 0 \quad x_D \to \infty, -\infty \le y_D \le \infty \; and \; t_D \ge 0 \tag{12}$$

$$C_D(x_D, y_D, t_D) \to 0 \quad y_D \to \infty, -\infty \le x_D \le \infty \; and \; t_D \ge 0 \tag{13}$$

$$C_D(x_D, y_D, t_D) = S_0 f(t_D, y_D) x_D = -\frac{U_x t}{R\sqrt{\frac{U_x R}{dD_x}}}, \tag{14}$$

$$-M_D \le y_D \le M_D \; and \; t_D = 0$$

$$C_D(x_D, y_D, 0) = 0 \quad 0 < x_D < \infty, -\infty \le y_D \le \infty \; and \; t_D = 0 \tag{15}$$

In the next subsection, Equations 11 - 15 will be resolved analytically by applying Green's function method.

3. Mathematical Solution Using Green's Function

The numbers of the pollutant level at position (x, y, t) within the region bounded by the river and the pumping well are represented by Green's function in this issue. The following integration can be solved in order to arrive at the answer of Equation 4.11 assuming that the river is situated at the line:

$$C_D(x^*{}_D, y_D, t_D) = \int_0^{t_D} -C_{wD}(\tau_D)\delta(x_D - L_D)\delta(y_D)G(x_D, y_D, \tau_D, x_{0_D}, y_{0_D})d\tau_D, \tag{16}$$

By deriving the equation below, we can yield G that is referred to as the Green's Function:

$$\frac{\partial^2 G}{\partial {x_D}^2} + \frac{\partial^2 G}{\partial {y_D}^2} - \frac{\partial G}{\partial t_D} = \delta(x_D - L_D)\delta(y_D)\delta(t_D) \tag{17}$$

According to Carslaw and Jaeger (1986) and Park and Zhan (2001), the one-dimensional Green's function is provided as follows:

$$G(X_D, t_D) = 1/\left(2\sqrt{\pi t_D}\right) exp(-{X_D}^2/(4\, t_D)) \tag{18}$$

The Green's function along the extended y-axis will undergo integration within this interval, as the pumping well's influence on the river is limited to the interval from -M to M. The resulting expression can be represented as follows:

$$S(Y_D, t_D) = \int_{-M_D}^{M_D} G(y_D - \zeta_D, t_D) = \int_{-M_D}^{M_D} 1/\left(\frac{2\sqrt{\pi t_D}\, exp(-(y_D - \zeta_D)^2}{4t_D}\right) d\zeta_D$$
$$= \frac{1}{2}\left(erfc((y_D - M_D)/(2\sqrt{t_D})) - erfc((y_D + M_D)/(2\sqrt{t_D}))\right) \tag{4.19}$$

The expression of the two-dimensional Green's function can be obtained by multiplying two one-dimensional Green's functions:

$$G(x_D, y_D, t_D) = G(x_D - L_D, t_D)S(y_D, t_D) \tag{20}$$

As a result, the following solution can be found:

$$C_D = \int_0^{t_D} -C_{wD}(\tau_D)\delta(x_D - L_D)\delta(y_D)G((x_D, y_D, \tau_D, x_{0_D}, y_{0_D})d\tau_D$$
$$= -1/\left(4R\sqrt{\pi}\right)q/Q \int_0^{t_D} 1/\sqrt{\tau_D} \exp\left(-(x_D - L_D)^2/(4\tau_D)\right)(erfc$$
$$((y_D + M_D)/(2\sqrt{t_D})) - erfc((y_D - M_D)/(2\sqrt{t_D})))d\tau_D \tag{21}$$

which becomes:

$$C(x,y,t) = S_0/(4R\sqrt{\pi})q/Q\sqrt{d/U_x} \exp\left(-\beta t/R\right)$$
$$\int_0^t \frac{1}{\sqrt{\tau}} \exp\left(\frac{-\sqrt{R}(1/D_x\left(x - L - \frac{U_x\tau}{R}\right)^2)}{4\tau}\right)$$
$$(erfc\left(\frac{\sqrt{R}(y - M)}{2\sqrt{D_y t}}\right) - erfc\left(\frac{\sqrt{R}(y + M)}{2\sqrt{D_y t}}\right) d\tau \tag{22}$$

4. Results and discussion

The numerical integration in Equation 22 is solved by using MATLAB. The governing equations were solved by using Green's function approach, and MATLAB software was used to calculate the numerical integration in the analytical solution and obtain the final solutions of. In the MATLAB software, various parameters is defined such as aquifer thickness, degradation factor, and dispersion coefficients along with its value. Table 1 below shows the summarization of all other input parameters used in the MATLAB.

Table 1: Input parameters used in the MATLAB software.

Parameter	Value
Leakance coefficient (λ)	0.1
Porosity (ϕ)	0.3
Longitude Dispersivity (a_l)	10 m
Transverse Dispersivity (a_t)	$0.1a_l$
Vertical Dispersivity (a_v)	$0.01a_l$
Initial concentration of contaminants (C_0)	16 mg/l
Aquifer thickness (d)	20 m
Storage coefficient (S_x)	0.7
Transmissivity (T)	2800 m^2/d
Degradation factor (β)	0.04 1/d
Pumping time (t_p)	200 d
Pumping rate (Q)	3075 m^3/d
Distance between the pumping well and river (L)	40 m

a) Examine The Influence of Pumping Time

Figure 2 illustrates the presence of pollutants within the defined region at various pumping time intervals. Different durations of pumping, namely 7, 14, 21, and 30 days, were tested. The contour plot was generated by applying all the parameter values in Table 1. The contour plot reveals that as the pumping time increases, the concentration of contaminants also increases. This can be attributed to the broader spread of contamination throughout the area. The observed increase in contaminant concentration can be attributed to the continuous flow of contaminants from the river. These contaminants are carried by the groundwater and transported toward the pumping well. As the pumping continues, more contaminated groundwater is drawn towards the well, resulting in a higher concentration of contaminants in the extracted water. This continuous flow of contaminants from the river introduces a constant source of pollutants, leading to the gradual accumulation and dispersion of contaminants in the aquifer. Therefore, the prolonged pumping duration allows for a more significant influx of contaminants into the aquifer, contributing to the higher concentration observed at the monitoring point.

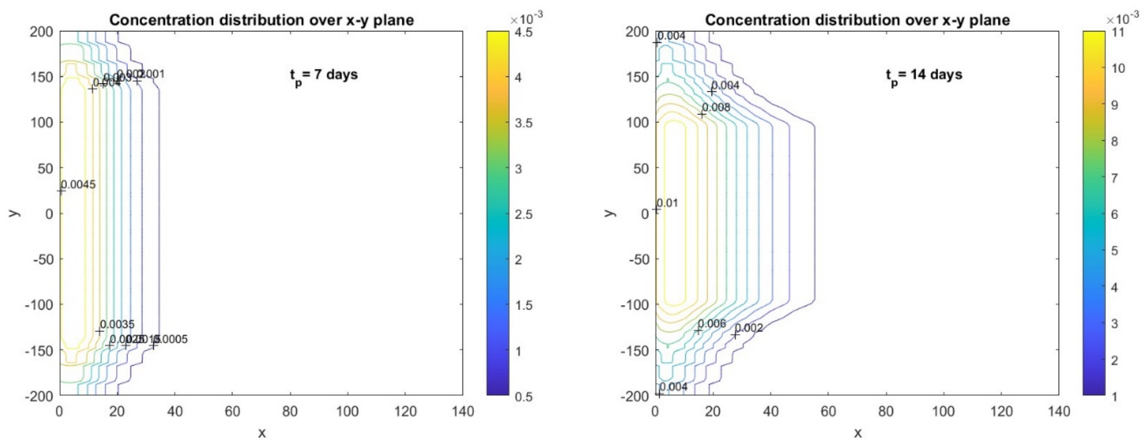

(a) (b)

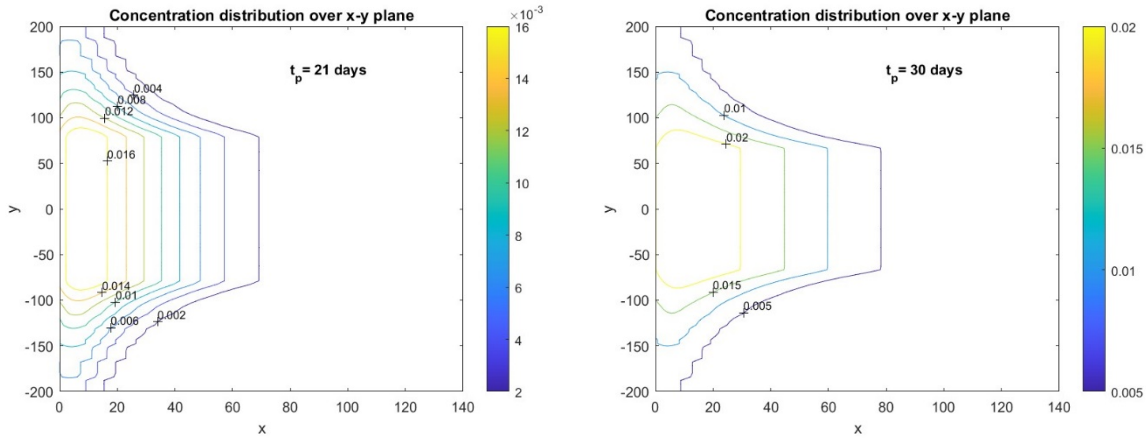

(c) (d)

Figure 2 The impact of pumping time on the concentration through contour plots. (a) $t_p = 7\ days$ (b) $t_p = 14\ day$s (c) $t_p = 21\ days$ (d) $t_p = 30\ days$ Schematic depiction of the pumping well from the river

b) Examine The Influence of Location of the Pumping Well

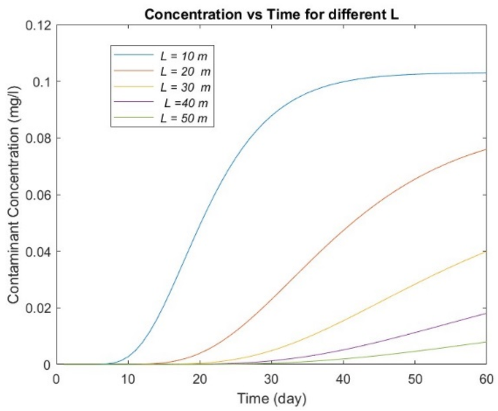

Figure 3 Plotting of contamination at different locations of pumping well

Figure 3 shows the concentration of a contaminant at different *L* values which are 10, 20, 40, and 50 m from the river edge using a pumping rate of 3075 m3/d. We consider all the parameter values in Table 1. Different value of L was chosen to investigate its influence on the contaminant transport process. The choice of different L values allowed for an exploration of how the concentration profiles change over time at various distances from the pumping well. The concentration profiles in Figure 4.3 illustrate how the contaminant concentration changes over time at different distances from the pumping well. As the location of the pumping well (L) parameter increases, the concentration of contaminants exhibits a more rapid and significant decrease over time. Higher length values result in lower concentrations at the same time intervals. When the location of the pumping well is farther away from the river, the contaminant concentration tends to decrease due to several factors. Firstly, as the distance increases, the groundwater has more time and space to attenuate and naturally dilute the aquifer contaminants. This natural attenuation occurs through dispersion, diffusion, sorption, and microbial degradation.

c) Examine The Influence of Pumping Rates

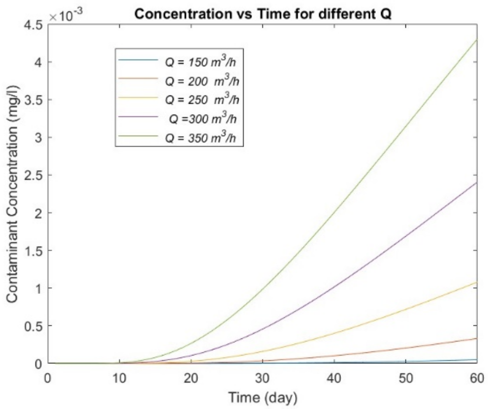

Figure 4 Plotting of contamination at different pumping rates

Figure 4 presents the level of a contaminant at five distinct values of the Q. We consider all the parameter values in Table 1 but with different value of L and Q where $L = 20$ m and $t_p = 60$ days. Different value of Q was chosen to investigate its influence on the contaminant transport process. The choice of different Q values allowed for an exploration of how the concentration profiles change over time at various pumping rates. Assuming a pumping well located 20 meters from the river, Figure 4 depicts the evaluation of pumping rates after 60 days. Based on the graph, the concentration of contamination varies with time for each pumping rate. The trend of the graph shows that as the pumping rate increases, the concentration of contamination increases. When the pumping rate increases, it suggests that more contaminant is being introduced into the system over time.

As a result, the concentration of the contaminant in the system increases because more of it is being transported. The higher pumping rate can also lead to faster flow velocities within the system. This increased velocity enhances the dispersion and mixing of the contaminant, causing it to spread out more evenly throughout the system. The bacteria present in the aquifer do not have sufficient time to mitigate and attenuate the rapid spread of pollution caused by high pumping rates, resulting in the swift manifestation of its impacts. Consequently, the concentration becomes more pronounced and measurable at different locations. In summary, the increased pumping rate results in a higher concentration of the substance due to the more significant amount being introduced and the improved dispersion caused by the higher flow velocities.

d) Examine the influence of Aquifer Thickness

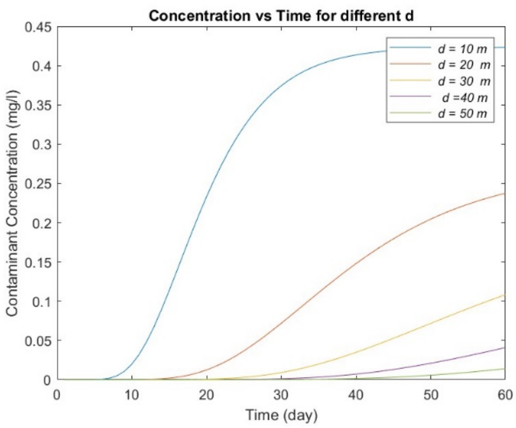

Figure 5 Plotting of contamination at different aquifer thickness

Figure 4.5 shows the concentration of contamination plotted over time at different aquifer thicknesses, d. Five different values of aquifer thickness were considered as shown in Figure 4.5. We consider all the parameter values in Table 1 but with different value of L where L=20 m. Different value of d was chosen to investigate its influence on the contaminant transport process. The choice of different d values allowed for an exploration of how the concentration profiles change over time at various aquifer thickness. As observed from the graph, the concentration of contamination varies with time for each aquifer thickness. Overall, the plots demonstrate that as the aquifer thickness increases, the rate of concentration increase over time becomes slower. This suggests that a thicker aquifer provides more space for the contaminant to disperse and dilute, resulting in a reduced impact and slower contamination rate.

Conclusion

The collected findings verified the model's usefulness for predicting the spread of contamination in a two-dimensional space. A contour map was used to visualize the outcomes for various pumping times. According to the results of contour plots for different pumping times, pollution concentration is proportionally correlated with pumping time. In other words, the contamination will keep spreading over a larger region in the direction of the well as the pumping time lengthens. Additionally, it is found that increasing the pumping rates can cause a considerable increase in contamination around the well. The system may experience faster flow velocities because of the higher pumping rate. The pollutant disperses and mixes more effectively due to the higher velocity, which leads to more even distribution throughout the system. The aquifer's resident bacteria need more time to slow down or stop the rapid development of contamination brought on by high pumping rates. Therefore, because more pollution is introduced at a time and is dispersed more effectively due to increased flow rates, the concentration of the contamination rises as the pumping rate increases.

Moreover, by increasing the location of the pumping well, the contaminant concentration will decrease. Because of a few circumstances, the concentration of contaminants tends to be lower when the pumping well is located farther from the river. First, as the distance grows, the groundwater has more space and time to attenuate and naturally dilute the aquifer contaminant. Dispersion, diffusion, sorption, and microbial degradation are some of the mechanisms that cause this natural attenuation. The last parameter that has been investigated is the aquifer thickness. As aquifer thickness increases, the growth rate in contaminant concentration becomes slower. This suggests that as aquifer thickness increases, the contaminant concentration will decrease. A thicker aquifer provides more space for the contaminant to disperse and dilute, resulting in a reduced impact and slower contamination rate.

References

[1] Adimalla, N., & Qian, H. (2020). Geospatial distribution and potential noncarcinogenic health risk assessment of nitrate contaminated groundwater in southern India: A case study. *Archives of Environmental Contamination and Toxicology*, *80*(1), 107–119. https://doi.org/10.1007/s00244-020-00762-7

[2] Canada, E. and C. C. (2017, June 9). *Government of Canada*. Canada.ca. Retrieved January 26, 2023, from https://www.canada.ca/en/environment-climate-change/services/water-overview/pollution-causes-effects/groundwater-contamination.html

[3] Chaubey, J., & Arora, H. (2017). Transport of contaminants during groundwater surface water interaction. *Water Science and Technology Library*, 153–165. https://doi.org/10.1007/978-3-319-55125-8_13

[4] Chen, J.-S. (2010). Analytical model for fully three-dimensional radial dispersion in a finite-thickness aquifer. *Hydrological Processes*, *24*(7), 934–945. https://doi.org/10.1002/hyp.7541

[5] Chen, K., & Zhan, H. (2018). A Green's function method for two-dimensional reactive solute transport in a parallel fracture-matrix system. *Journal of Contaminant Hydrology*, *213*, 15–21. https://doi.org/10.1016/j.jconhyd.2018.03.006

[6] Keesari, T., Pant, D., Roy, A., Sinha, U. K., Jaryal, A., Singh, M., & Jain, S. K. (2021). Fluoride geochemistry and exposure risk through groundwater sources in northeastern parts of Rajasthan, India. *Archives of Environmental Contamination and Toxicology*, *80*(1), 294–307. https://doi.org/10.1007/s00244-020-00794-z

[7] Lasagna, M., De Luca, D. A., & Franchino, E. (2016). Nitrate contamination of groundwater in the Western Po Plain (Italy): The effects of groundwater and surface water interactions. *Environmental Earth Sciences*, *75*(3). https://doi.org/10.1007/s12665-015-5039-6

[8] Le, D. V., Giang, P. T., & Nguyen, V. T. (2022). Investigation of arsenic contamination in groundwater using hydride generation atomic absorption spectrometry. *Environmental Monitoring and Assessment*, *195*(1). https://doi.org/10.1007/s10661-022-10707-3

[9] Lee, C.-M., Hamm, S.-Y., Yun, S.-M., Oh, J.-E., Kim, M. S., & Kim, H. (2018). Indication of groundwater contamination using acesulfame and other pollutants in a rural area of Korea. *Water*, *10*(12), 1731. https://doi.org/10.3390/w10121731

[10] Li, P., Karunanidhi, D., Subramani, T., & Srinivasamoorthy, K. (2021). Sources and consequences of groundwater contamination. *Archives of Environmental Contamination and Toxicology*, *80*(1), 1–10. https://doi.org/10.1007/s00244-020-00805-z

[11] Mahdavi, A. (2015). Transient-state analytical solution for groundwater recharge in anisotropic sloping aquifer. *Water Resources Management*, *29*(10), 3735–3748. https://doi.org/10.1007/s11269-015-1026-7

[12] Mahdavi, A. (2020). Steady-state response of annular wedge-shaped aquifers to arbitrarily-located multiwells with regional flow. *Journal of Hydrology*, *586*, 124906. https://doi.org/10.1016/j.jhydrol.2020.124906

[13] Mahdavi, A. (2021). Hydrological components of groundwater recharge in leaky aquifers adjacent to semipervious Streambank: Analytical study. *Environmental Science and Pollution Research*, *29*(17), 24833–24848. https://doi.org/10.1007/s11356-021-17468-5

[14] Mahdavi, A., & Seyyedian, H. (2013). Transient-state analytical solution for groundwater recharge in triangular-shaped aquifers using the concept of expanded domain. *Water Resources Management*, *27*(8), 2785–2806. https://doi.org/10.1007/s11269-013-0315-2

[15] Mustafa, S., Bahar, A., Aziz, Z. A., & Suratman, S. (2016). Modelling contaminant transport for pumping wells in Riverbank Filtration Systems. *Journal of Environmental Management*, *165*, 159–166. https://doi.org/10.1016/j.jenvman.2015.09.026

[16] Mustafa, S., Bahar, A., Zainal Abidin, A. R., Abdul Aziz, Z., & Darwish, M. (2021). Three dimensional model for solute transport induced by groundwater abstraction in river-aquifer systems. *Alexandria Engineering Journal*, *60*(2), 2573–2582. https://doi.org/10.1016/j.aej.2020.12.053

[17] Paladino, O., Moranda, A., Massabò, M., & Robbins, G. A. (2017). Analytical solutions of three-dimensional contaminant transport models with exponential source decay. *Groundwater*, *56*(1), 96–108. https://doi.org/10.1111/gwat.12564

[18] Prunes, E. H. & E. (2022, March 21). *What is groundwater and why is it so important?* WWF. Retrieved January 26, 2023, from https://www.worldwildlife.org/stories/what-is-groundwater-and-why-is-it-so-important

[19] Sajedi-Hosseini, F., Malekian, A., Choubin, B., Rahmati, O., Cipullo, S., Coulon, F., & Pradhan, B. (2018). A novel machine learning-based approach for the risk assessment of nitrate groundwater contamination. *Science of The Total Environment*, *644*, 954–962. https://doi.org/10.1016/j.scitotenv.2018.07.054

[20] Secomb, T. W. (2015). A Green's function method for simulation of time-dependent solute transport and reaction in realistic microvascular geometries. *Mathematical Medicine and Biology*, *33*(4), 475–494. https://doi.org/10.1093/imammb/dqv031

[21] Secomb, T. W. (2015). A Green's function method for simulation of time-dependent solute transport and reaction in realistic microvascular geometries. *Mathematical Medicine and Biology*, *33*(4), 475–494. https://doi.org/10.1093/imammb/dqv031

[22] Selvakumar, S., Chandrasekar, N., & Kumar, G. (2017). Hydrogeochemical characteristics and groundwater contamination in the rapid urban development areas of Coimbatore, India. *Water Resources and Industry*, *17*, 26–33. https://doi.org/10.1016/j.wri.2017.02.002

[23] Shah, T., Molden, D., Sakthivadivel, R., & Seckler, D. (2000). The Global Groundwater Situation: Overview of opportunities and challenges. https://doi.org/10.5337/2011.0051

[24] Stanev, V. G., Iliev, F. L., Hansen, S., Vesselinov, V. V., & Alexandrov, B. S. (2018). Identification of release sources in advection–diffusion system by machine learning combined with Green's function inverse method. *Applied Mathematical Modelling*, *60*, 64–76. https://doi.org/10.1016/j.apm.2018.03.006

[25] Syafiuddin, A., Boopathy, R., & Hadibarata, T. (2020). Challenges and solutions for sustainable groundwater usage: Pollution Control and Integrated Management. *Current Pollution Reports*, *6*(4), 310–327. https://doi.org/10.1007/s40726-020-00167-z

[26] Water Science School. (2018). *Contamination of groundwater* . Contamination of Groundwater | U.S. Geological Survey. Retrieved December 27, 2022, from https://www.usgs.gov/special-topics/water-science-school/science/contamination-groundwater

[27] Woodard, J. (2021). *What is groundwater contamination and how do you treat it?* Fresh Water Systems. Retrieved December 11, 2022, from https://www.freshwatersystems.com/blogs/blog/what-is-groundwater-contamination-and-how-do-you-treat-it

[28] Zhan, H., Wen, Z., & Gao, G. (2009). An analytical solution of two-dimensional reactive solute transport in an aquifer-aquitard system. *Water Resources Research*, *45*(10). https://doi.org/10.1029/2008wr007479

[29] Li, S., Li, J., Dong, M., Fan, S., Zhao, T., Wang, J., & Fan, W. (2019). Strategies to control zeolite particle morphology. *Chemical Society Reviews*, 48(3), 885-907.

[30] Petrov, A. W., Ferri, D., Kröcher, O., & van Bokhoven, J. A. (2019). Design of stable palladium-based zeolite catalysts for complete methane oxidation by postsynthesis zeolite modification. *ACS Catalysis*, 9(3), 2303-2312.